The 3 . 4 μ m absorption in Titan's stratosphere: Contribution of ethane, propane, butane and complex hydrogenated organics

T. Cours, D. Cordier, B. Seignovert, L. Maltagliati, Ludovic Biennier

- A strong and unexplained absorption at 3.4 μm in Titan's atmosphere has been revealed by solar occultations by the instrument CASSINI/VIMS

- Several simple molecules (like CH_4 or C_2H_6) absorb in this region but their effect is not efficient enough to account for observations

- We show that Polycyclic Aromatic Hydrocarbon (PAH) or Hydrogenated Amorphous Carbons (HAC) could be introduced to reproduce this band

The 3.4 μm absorption of the Titan's stratosphere: contribution of ethane, propane, butane and complex hydrogenated organics

T. Cours[a], D. Cordier[a], B. Seignovert[a,b], L. Maltagliati[c], L. Biennier[d]

[a] *Université de Reims Champagne Ardenne, CNRS, GSMA UMR 7331, 51097 Reims, France*
[b] *Jet Propulsion Laboratory, California Institute of Technology, 4800 Oak Grove Dr, MS 183-501, Pasadena, CA 91109, USA*
[c] *Nature Astronomy, Springer Nature, 4 Crinan Street, N1 9XW London, UK*
[d] *Institut de Physique de Rennes, Département de Physique Moléculaire, Astrophysique de Laboratoire, UMR CNRS 6251, Université de Rennes 1, Campus de Beaulieu, 35042 Rennes Cedex – France*

Abstract

The complex organic chemistry harbored by the atmosphere of Titan has been investigated in depth by Cassini observations. Among them, a series of solar occultations performed by the VIMS instrument throughout the 13 years of Cassini revealed a strong absorption centered at ~ 3.4 μm. Several molecules present in Titan's atmosphere create spectral features in that wavelength region, but their individual contributions are difficult to disentangle. In this work, we quantify the contribution of the various molecular species to the 3.4 μm band using a radiative transfer model. Ethane and propane are a significant component of the band but they are not enough to fit the shape perfectly, then we need something else. Polycyclic Aromatic Hydrocarbons (PAHs) and more complex polyaromatic hydrocarbons like Hydrogenated

Email address: thibaud.cours@univ-reims.fr (T. Cours)

Amorphous Carbons (HACs) are the most plausible candidates because they are rich in C-H bonds. PAHs signature have already been detected above $\sim$ 900 km, and they are recognized as aerosols particles precursors. High similarities between individual spectra impede abundances determinations.

Keywords: planets and satellites: individual: Titan – planets and satellites: general – solar system: general

1. Introduction

Titan is an extraordinary object among the planets and satellites of the solar system. Its thick atmosphere, mainly composed of nitrogen and methane, harbors a complex photochemistry producing organic compounds that participate to the formation of haze which produces its typical orange/brown color. Due to its unique and exotic properties, Titan's atmosphere remains a very active field of research in investigating the possible origin and main properties (Johnson *et al.*, 2016; Charnay *et al.*, 2014; Newman *et al.*, 2016). Its composition can be modeled by complex chemical network (Krasnopolsky, 2014; Lavvas *et al.*, 2015), but also by laboratory experiments (Bourgalais *et al.*, 2016; Romanzin *et al.*, 2016) to match the observations made by Cassini's instruments (Vinatier *et al.*, 2015; Coustenis *et al.*, 2016; Bellucci *et al.*, 2009). In Bellucci *et al.* (2009), the authors raised an issue about the CH_4 3.3 μm band.

In 2006, during Cassini's 10^{th} flyby of Titan (T10), Bellucci *et al.* (2009) observed features in CH_4 3.3 μm band with the Visible and Infrared Mapping Spectrometer (VIMS). VIMS is an imaging spectrometer onboard the Cassini spacecraft. This instrument is composed of a visible channel ($0.3 - 1.05$ μm) and a infrared channel ($0.89 - 5.1$ μm). The FWHM of the 256 infrared spectral pixels are in the range 13 - 20 nm. VIMS can be used in different observation modes corresponding to nadir, limb and occultation geometry. Our study use the latter mode. More details can be found in Maltagliati *et al.* (2015). Bellucci *et al.* (2009) tentatively attributed the observed features in CH_4 3.3 μm band to solid state organic compounds, similar to those observed in the InterStellar Medium (ISM) (Sandford *et al.*, 1991; Pendleton

& Allamandola, 2002). However, this interpretation was far to be firm and Bellucci *et al.* (2009) concluded that precise comparison of their data with laboratory spectrum needed in future work.

Interestingly, a similar feature had been observed by VIMS during a stellar occultations in Saturn's atmosphere (Nicholson *et al.*, 2006; Kim *et al.*, 2012). Continued by Kim *et al.* (2012), these analysis shown that the optical-depth spectra exhibit a broad peak at 3.36-3.41 μm for the observations obtained at 12 pressure levels between 0.0150 and 0.0018 mbar in the Saturnian atmosphere. Kim *et al.* (2012), in particular, attributed these 3.4 μm spectral features to the aliphatic C–H stretching bands of solid-state hydrocarbons, such as C_5H_{12}, C_6H_{12}, C_6H_{14} and C_7H_{14}. Kim *et al.* (2011) reached a similar conclusion for Titan in analyzing the occultation T10. However, the formation of such organic microcrystals in the atmosphere of Titan is questionable due to thermodynamic arguments (see Sec. 2).

More recently, Maltagliati *et al.* (2015) analyzed an extended set of four VIMS solar occultations, performed between January 2006 and September 2011. In Fig. 1, we reporte an example of transmission data derived from Maltagliati *et al.* (2015). Spectra have been normalized by a 3^{th} order polynomial and data have been interpolated at the altitude of 145 km to allow easy comparisons. This value offers a good compromise: at lower altitudes, the stronger absorptions damp spectral features and at higher altitudes, the absorptions are weak and the spectra are more noisy due to a weaker signal. Deviations between the four curves ploted in Fig. 1 give an idea of transmittance uncertainties, and spatial or temporal variations in Titan's atmosphere.

Table 1: Triple points coordinates for the sample of hydrocarbon species considered by Kim *et al.* (2011). The temperatures have all been taken in the NIST database†, for CH_3CN, C_5H_{12} and C_6H_{12}. The pressures are not available in this database, we then estimated their values by using their Antoine's equation at the triple point temperature.

Species	Chemical formula	$T_{\rm triple}$ (in K)	$P_{\rm triple}$ (in bar)
Ethane	C_2H_6	91.0	1.1×10^{-5}
Methane	CH_4	90.7	1.2×10^{-1}
Methylcyanide	CH_3CN	229.3	2.2×10^{-3} *
Pentane	C_5H_{12}	143.5	3.9×10^{-7} *
Cyclohexane	C_6H_{12}	279.7	5.3×10^{-2} *

†http://webbook.nist.gov/chemistry/

* Our estimation

In their line-by-line radiative transfer model, Maltagliati *et al.* (2015) took into account the absorption caused by 9 molecules : CH_4 , CH_3D, CO, CO_2, C_2H_2, C_2H_4, C_2H_6, HCN and N_2. In spite of the level of sophistication of their approach, Maltagliati *et al.* (2015) found a clear disagreement between the observed absorption in the 3.4 μm band and their computed spectra. It appears then that the atmosphere of Titan is a more efficient absorber than in this model. By comparing the observed residual absorption and the ethane cross sections measured by the Pacific Northwest National Lab (PNNL - Sharpe *et al.*, 2004), and given the lack of C_2H_6 spectral lines in major databases (HITRAN and GEISA), Maltagliati *et al.* (2015) interpreted the strong absorption band centered at 3.4 μm as the effect of ethane. These authors also tentatively attribute the narrow absorption at 3.28 μm

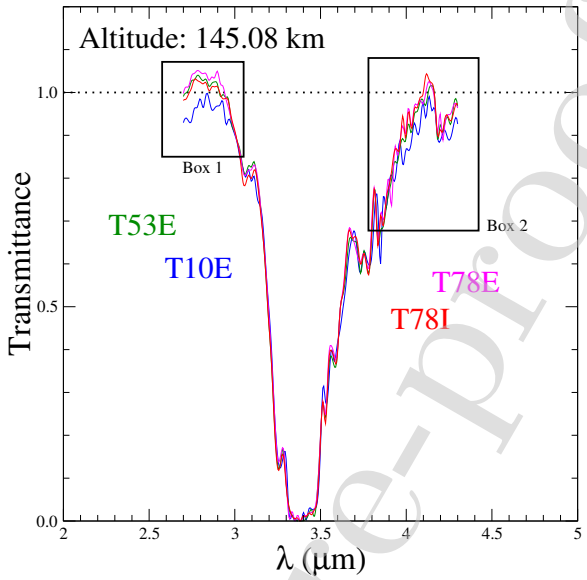

Figure 1: Transmittance curves derived from solar occultations T10E, T53E, T78E and T78I studied by Maltagliati *et al.* (2015). Altitude interpolations, at 145 km, have been performed to allow easy comparisons. Boxes delineate domains where data are significantly noisy.

to the presence of Polycyclic Aromatic Hydrocarbons (PAHs) in the stratosphere. Indeed, a few years before, López-Puertas *et al.* (2013) identified the presence of these aromatic molecules in Titan's upper atmosphere around 650 km up to $\sim$ 1300 km. Their results rely on the emission near 3.28 μm detected by VIMS.

It is well accepted that a strong absorption at $3.2 - 3.5$ μm is related to the C-H stretching bands, but the C-H bonds can be present in icy hydrocarbons, in simple molecules, in more complex polyaromatic hydrocarbons

or in aerosols particles. In this paper, we try to disentangle the problematic attribution of this strong absorption around 3.4 μm. In Fig 1, transmittances corresponding to box 1 and box 2 are clearly too noisy to allow a clear analysis. In this work, we specifically focus our efforts on the highest absorption spectral range, *i.e.* between 3.3 and 3.5 μm. In Sec. 2 we examine, in the light of an advanced thermodynamic model, the possibility of the existence of hydrocarbon ices in the stratosphere of Titan, as proposed by Kim *et al.* (2011). In Sec. 3 and 4 we revisit the absorption of gases in the 3.4 μm spectral region while in Sec. 5 we discuss the possible presence of PAHs or more complex polyaromatic hydrocarbons like Hydrogenated Amorphous Carbons (HACs). In Sec. 6, we further discuss these issues and present our conclusions.

2. Solid-Vapor equilibria in Titan's stratosphere

An explanation for the nature of Titan's 3.4 μm absorption was put forward by Kim *et al.* (2011) who could reproduce the VIMS solar occultations by using hydrocarbon ices like C_2H_6, CH_4, CH_3CN, C_5H_{12} and C_6H_{12} ices. However, the real existence of such ices in the stratosphere of Titan needs to be discussed. Indeed, as mentioned by Kim *et al.* (2011), above 130 km (the lowest altitude explored by these authors) the temperature remains in $160 - 190$ K interval while the pressure decreases below 5×10^{-3} bar. A look at Table 1, in which we have gathered the triple points coordinates of involved species, shows that at least C_2H_6, CH_4 and C_5H_{12} should not be in solid form at these relatively high temperatures. In order to investigate more

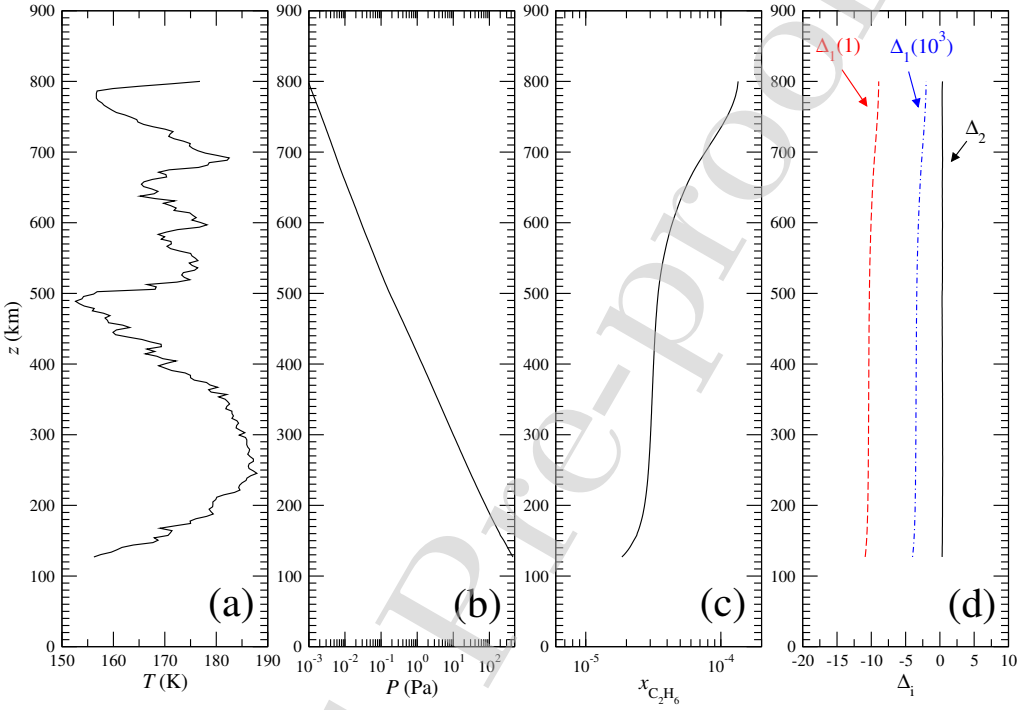

Figure 2: Panels (a) and (b) stand respectively for the temperature and pressure profiles, provided by HASI instruments, between the altitudes 127 km and 800 km in the atmosphere of Titan (Fulchignoni *et al.*, 2005). Panel (c) represents the molar fraction of ethane as computed by Lavvas *et al.* (2008a,b). In panel (d) the thermodynamic quantities Δ_1 and Δ_2 (defined in the text by Eq. (1) and Eq. (2)) for ethane. We recall that Δ_1 and Δ_2 correspond respectively to the chemical potential, of a given species, in the gas phase and in the solid phase, the coexistence of both is reached when $\Delta_1 = \Delta_2$ (see Eq. (3)). $\Delta_1(1)$ corresponds to the abundances found by Lavvas *et al.*'s while $\Delta_1(10^3)$ has been obtained by multiplying the mole fraction $x_{C_2H_6}$ by 10^3.

95 deeply the existence of these ices, we introduce two quantities, the first is:

$$\Delta_{1,i} = \ln\left(\Gamma_i^{\rm vap}\, y_i\right) \tag{1}$$

where y_i is the mole fraction of the compound i at equilibrium, in the vapor, and $\Gamma_i^{\rm vap}$ is the activity coefficient of the considered species. The second introduced term is written as :

$$\Delta_{2,i} = -\frac{\Delta H_{i,m}}{RT_{i,m}} \left(\frac{T_{i,m}}{T} - 1 \right) \tag{2}$$

The thermodynamic equilibrium between the species i in the vapor, and its icy counterpart , is reached when the equation :

$$\Delta_{1,i} = \Delta_{2,i} \tag{3}$$

is satisfied (Poling *et al.*, 2007). Eq. (3) correspond to a thermodynamic equilibrium between the considered organic ice i and the vapor – Eq. (3) is an equality of chemical potential. The activity coefficient $\Gamma_i^{\rm vap}$ is given by the Perturbed-Chain Statistical Associating Fluid Theory (PC-SAFT). Originally proposed by Gross & Sadowski (2001), PC-SAFT is now widely employed in the chemical engineering community, due to its very good performances. This theory has been successfully employed in several recent studies of Titan to model liquid-vapor and solid-liquid equilibria (Tan *et al.*, 2013; Luspay-Kuti *et al.*, 2015; Tan *et al.*, 2015; Cordier *et al.*, 2016; Cordier, 2016).

In Eq. (1) the activity coefficient $\Gamma_i^{\rm vap}$ quantifies the *degree of ideality* of the considered gas mixture. When $\Gamma_i^{\rm vap} \sim 1$ the system has an ideal behavior, *i.e.* all the molecules of the same species and those of different species interact with the same intensity. In our context, for all the molecules listed in Table 1, we found the $\Gamma_i^{\rm vap}$'s very close to unity, whatever the altitude. This indicates an ideal behavior of the gases, which is not a surprise at densities provided by HASI measurements (Fulchignoni *et al.*, 2005). Practically, this means that Eq. (3) can be satisfied only if $\Delta_{2,i}$ is negative,

meaning that the molar fraction y_i has to be smaller than unity. In the case of ethane, $\Delta_{2,i}$ remains slightly larger than zero (see Fig. 2.d), then, in the conditions of pressure and temperature in the Titan's stratosphere, according to the present model, C_2H_6 can never form solid particles. For the other species, even if $\Delta_{2,i} < 0$, the measured or estimated values of their mole fractions are order of magnitude too small for Eq. (3) to be satisfied. For instance, concerning CH_3CN, Lara *et al.* (1996) (see their Fig. 10 p. 279) reported abundances, derived from ground-based millimeter-wave observations (Bézard *et al.*, 1993), between roughly 10^{-9} and 10^{-7} in molar fraction, while Lavvas *et al.* (2008a,b) computed values around 10^{-8}. Our calculations show that even in the most favorable case (*i.e.* when the abundances of CH_3CN is taken equal to 10^{-7}) the term $\Delta_{1,i}$ is more than ten orders of magnitude smaller than the typical value of $\Delta_{2,i}$ in stratospheric conditions. As a consequence, we conclude that the compounds proposed by Kim *et al.* (2011) cannot exhibit solid-vapor equilibria in the stratosphere of Titan. The only possibility remaining is the presence of these icy hydrocarbon aerosols in a non-equilibrium state, but such a situation seems unlikely.

3. Radiative transfer modeling of the 3.4 μm absorption

In order to simulate the properties of the flux of photons that emerges from the Titan's atmosphere during a solar occultation, we have built a simple radiative transfer model. On one hand, the structure of the atmosphere is represented by a set of concentric spherical shells; on the other hand, the solar radiations are assumed to follow a straight optical path througth the atmosphere. The refraction is neglected in our entire approach, this approx-

imation is relevant due to the low density probed in these explored regions. For a given altitude z, the transmittance $T(\lambda, z)$ of the atmosphere at the wavelength λ is estimated using

$$T(\lambda, z) = \exp(-\sum_{i,j,k} N_j x_{i,j} \sigma_{i,k} l_j) \tag{4}$$

where the indexes i, j and k denote respectively the chemical species, the atmospheric layers and the spectral lines. The cross-sections are $\sigma_{i,k}$, N_j represents the total number of molecules (per units of volume) in layer j, while $x_{i,j}$ is the molar fraction of species i in the same layer. Finally l_j stands for the distance travelled by photons in the layer j (see Fig. 3). Doing several tests on the number of layers, we found $N_{\text{layers}} = 70$ to be a sufficient total number of shells, linearly distributed between the ground and a maximum altitude of 700 km. The pressure and temperature profiles come from HASI measurements (Fulchignoni *et al.*, 2005). The cross-section $\sigma_{i,k}$ (in cm^2/molecule) are written as

$$\sigma_{i,k}(\tilde{\nu}) = I_{i,k}(\tilde{\nu}_{i,k})\, f(\tilde{\nu} - \tilde{\nu}_{i,k}) \tag{5}$$

where f is a Voigt profile, $\tilde{\nu}$ and $\tilde{\nu}_{i,k}$ are respectively the wavenumber (in cm^{-1}) and the spectral line k wavenumber of the chemical species i, $I_{i,k}$ are the intensities (in cm/molecule) of the spectral line k of the chemical species i. In the cases where high resolution spectral data are available, the cross-section $\sigma_{i,k}$ are computed using $k-$correlated coefficient method (Arking & Grossman, 1972; Chou & Arking, 1980; Fu & Liou, 1992). When only low resolution spectral data are available in the literature or when the lines are wider than the spectral resolution of VIMS (16-20 nm), the $k-$correlated

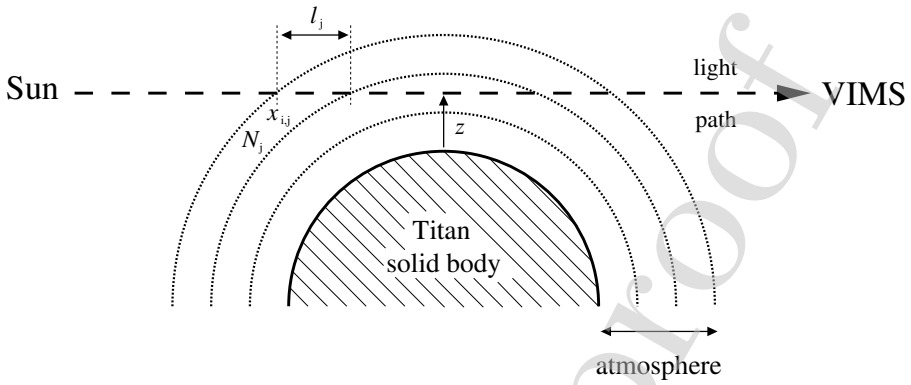

Figure 3: A schematic representation of our "onion-skin" radiative tranfer model, used in this paper and suitable for the analysis of Titan's solar occultations data published by Maltagliati *et al.* (2015). In the text, the term *altitude* refers to the parameter called "z" in this figure. After tests with different numbers of layers, a total number $N_{\text{layers}} = 70$ of atmospheric layers was found sufficient to describe the atmosphere. Layers have been linearly distributed between the ground and 700 km.

coefficient method is not necessary to compute cross-section and therefore a Gauss profile has been proved to be sufficient.

Our initial composition is based on the one published by Maltagliati *et al.* (2015) and include the following molecules : CH_4, CH_3D, CO, C_2H_2, C_2H_4, C_2H_6, H_2O, C_6H_6 and HCN. In this entire paper, we adopt this list of species as our First Guess composition (hereafter FG composition), the influence of other compounds will be made by comparing what it is obtained using this FG composition. Nitrogen is voluntarily omitted since it is extremely poor absorbant in the domain of interest. Moreover, the collision-induced effects are negligible within the band $3.3 - 3.5$ μm. The CH_4, C_2H_2, C_2H_4, C_2H_6, C_6H_6 and HCN vertical mixing ratio profiles come from photochemical models developed by Krasnopolsky (2014). The abundance of deuterated

methane (CH_3D) with respect to the methane has been kept constant with a CH_3D/CH_4 ratio of about 5.3×10^{-4} (Bézard *et al.*, 2007). Concerning water, we performed tests including molar fractions corresponding to the highest value given by Coustenis *et al.* (1998). Finally, the abundance of CO has been taken from Flasar *et al.* (2005).

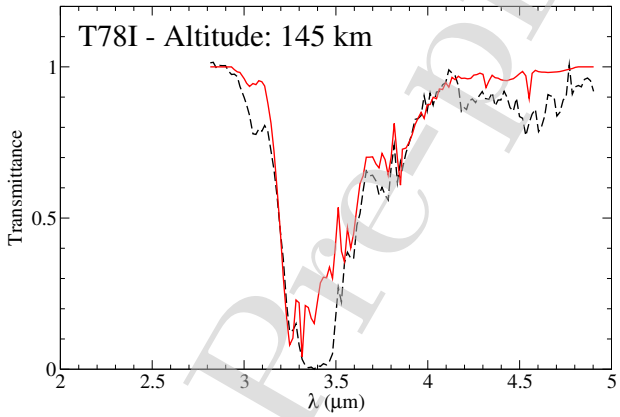

Figure 4: Comparison between observed transmittance (dashed line) acquired during occultation T78I at the altitude of 145 km (Maltagliati *et al.*, 2015), and the computed transmittance due to our FG composition: with only CH_4, CH_3D, CO, C_2H_2, C_2H_4, C_2H_6, H_2O, C_6H_6 and HCN. For C_2H_6, only spectral lines provided by HITRAN have been taken into account.

The spectral data of CO, C_2H_2, H_2O and HCN were mainly taken in HITRAN[1] (Rothman *et al.*, 2013) and GEISA[2] (Jacquinet-Husson *et al.*, 2008). For CH_4, CH_3D and C_2H_4 we used the up-to-date theoretical line lists computed by Rey *et al.* (2016) and available at the Theoretical Reims-Tomsk

[1] http://hitran.org/
[2] http://www.pole-ether.fr/geisa/

Spectral database[3]. For benzene, due to the lack of data in these database, we performed *ab initio* computations of its absorption frequencies and their respective intensities. Based on the `MP2/6-311G**` level of the theory, developed by Moller & Plesset (1934), we obtained frequencies, which were scaled by 0.95, according to that is the recommended in such a situation. The only none zero intensities near the 3.4 μm band are for the frequencies 3064.0917 cm^{-1} (3.26 μm) and 3064.0949 cm^{-1} (3.26 μm) (including the scaling factor of 0.95) corresponding to two C-H asymmetric stretching normal modes. The intensities were found quite low with values of 32.63 km/mole for both transitions. Considering the vertical profile of C_6H_6, we find that the benzene is a minor absorber around 3.26 μm.

Maltagliati *et al.* (2015) selected a set of four occultations data, T10 Egress (T10E), T53 Egress (T53E), T78 Egress (T78E) and T78 Ingress (T78I) acquired during three flybys, T10, T53 and T78 respectively. For each occultation, the altitude ranges between $\sim$ 50 km and $\sim$ 690 km. We provide, in supplementary material, four cube's name lists used in our analysis, one name list by occultation. The name lists are in Excel cvs format and can be downloaded from the pds-rings site [4]. For all these occultations, the retrieved transmittance curves, at a given altitude, are extremely similar (see for instance Fig. 11 of Maltagliati *et al.*, 2015). In order to facilitate comparison between our theoretical output, and observational determinations, we have chosen the Ingress occultation T78 (T78I) as a typical case. We also selected the altitude of 145 km because it offers a good compromise between

[3] `http://theorets.tsu.ru`

[4] `https://pds-rings.seti.org/cassini/vims/`

high altitudes data for which the transmittance curves are pretty flat, and low altitudes measurements presenting a global strong absorption that masks or damps spectral features.

A first model-observation comparison can be seen in Fig. 4, the disagreement is clear, particularly around 3.4 μm our domain of interest. This nicely confirms the findings by Maltagliati *et al.* (2015).

4. The possible absorption of ethane, propane and butane around 3.4 μm

4.1. Ethane

As already mentioned, the C-H stretching bands produce a strong absorption at $3.2-3.5$ μm, this is why any compound containing one or several C-H bounds can potentially contribute to the observed 3.4 μm absorption. In this context, ethane, quantitatively the main product of Titan's photochemistry (Lavvas *et al.*, 2008a,b; Krasnopolsky, 2014), should be the object of our first intentions. The presence of ethane in the Titan's atmosphere is firmly established by previous observations, *e.g.* it has been detected by Cassini's instruments: UVIS (Koskinen *et al.*, 2011), INMS (Cui *et al.*, 2009) and CIRS (Vinatier *et al.*, 2010). Unfortunately, in HITRAN and GEISA databases, ethane spectral lines in the band of interest are pretty scarce. Surprisingly, the absorption spectrum of the C-H stretching region of ethane, measured by Pine & Lafferty (1982) (hereafter PL82) at T= 119 K, is not available in these compilations. Then, we included the $\sim$ 3000 lines provided by PL82 data in our model; 1614 entries specify wavenumbers, intensities and the lower state energies whereas for 1426 other entries the lower state energy is

not available. Thus, in the latter case, we have neglected the temperature corrections of the intensities. The contribution to the absorption around 3.4 μm, of ethane alone, is plotted in Fig. 5(a).

Unfortunately, Pine & Lafferty (1982) did not include ethane PQ-branches which should have a non-negligible contribution in the domaine of interest. To tackle the issue, we used an empirical pseudo-line list based on the cross-section measurements developed by Harrison *et al.* (2010) (hereafter H10 dataset) and freely available on the web[5]. Compared to the absorption obtained with PL82 spectral lines, the effect of ethane is significantly enhanced by the use of this more comprehensive list (Fig. 5.b). If both, the PL82 and H10 spectral data, are simultaneously included in our model (Fig. 5.c), the actual effect of PL82 is not noticeable. Finally, if we merge PL82 and H10 spectral lines sets, with those employed for our FG composition model, the disagreement with Cassini/VIMS observations is considerably reduced (Fig. 5.d). This clearly demonstrates the prominent role of ethane, as an absorber, at wavelengths around 3.4 μm. Nonetheless, the simulated transmittance remains significantly above the observed one. This fact suggests the presence of other absorbers, possibility which we discuss further in next paragraphs.

4.2. Propane

According to photochemical models (Lavvas *et al.*, 2008a,b; Krasnopolsky, 2014), propane should also be produced in Titan's upper-atmosphere. This C_3 hydrocarbon has been detected by several Cassini's instruments:

[5] http://mark4sun.jpl.nasa.gov/pseudo.html

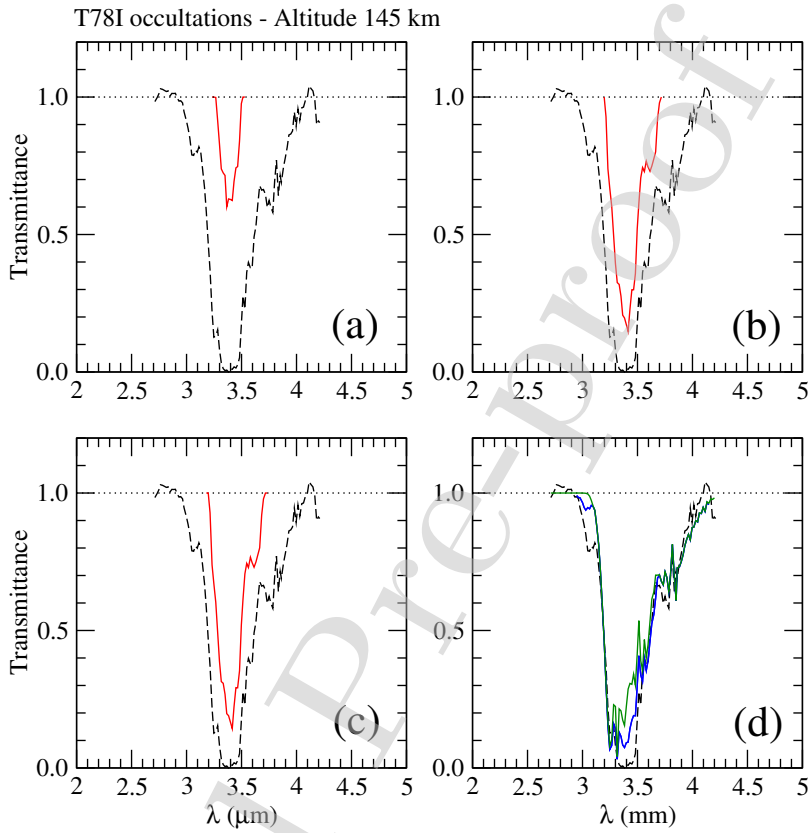

Figure 5: Comparison between simulated transmittances and VIMS for the T78I occultation data (Maltagliati *et al.*, 2015). Observational data are in dashed line, the altitude is 145 km. This figure shows the transmittance of C_2H_6 using: (a) only Pine & Lafferty (1982) spectral lines (red), (b) only pseudo-lines lists based on the cross-section measurements (Harrison *et al.*, 2010) (red), (c) the combination of PL82 and H10 spectral data (red), (d) the combination of our FG composition model with PL82 and H10 (blue), the absorption computed with our FG composition is also plotted for comparison (green solid line).

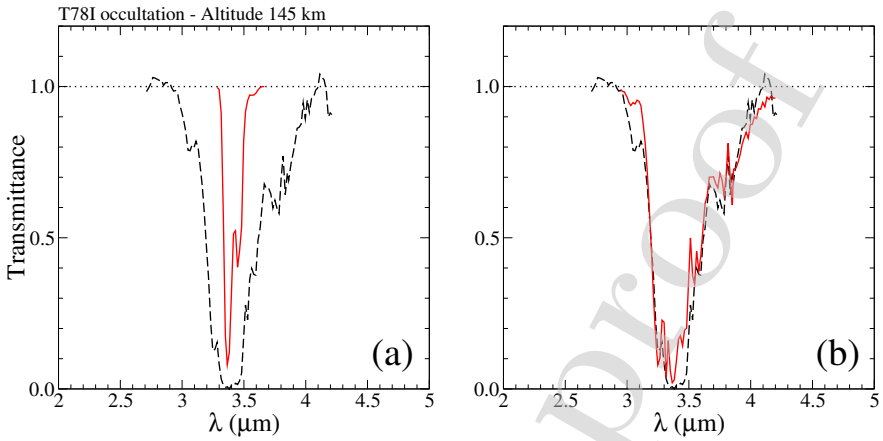

Figure 6: Occultation T78I at 145 km (observed transmittance in dash line) : (a) Absorption due to propane alone, (b) computed absorption using our FG composition complemented by propane (ethane is not taken into account).

Nixon *et al.* (2013) determined its mixing ratio using CIRS, while Cui *et al.* (2009) and Magee *et al.* (2009) retrieved abundances from INMS measurements. Similarly to the ethane case, HITRAN and GEISA are very poor in spectral data around 3.4 μm for this molecule. Then, we used the propane pseudo-lines list based on the cross-section measurements of Harrison & Bernath (2010) (freely available on the web[6]). Taking into account the propane abundance profil predicted by Krasnopolsky (2014), we have estimated the corresponding absorption in our domain of interest: in Fig. (6) we have displayed the absorption of propane alone a), the effet of this molecule is combined with that of our FG composition sample b), clearly the contribution of propane is comparable to that of ethane, even is propane is

[6] http://mark4sun.jpl.nasa.gov/pseudo.html

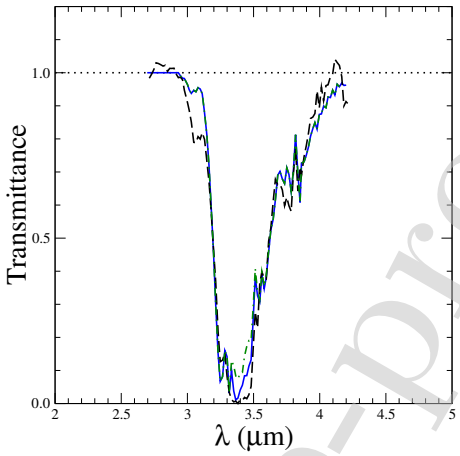

Figure 7: Dashed line : T87I observations, dot-dashed line: our computation taking into account gases of our FG composition and ethane (including pseudo-lines and Lafferty data), solid line: the same simulation including propane pseudo-lines list based on the cross-section measurements of Harrison & Bernath (2010).

approximately one order of magnitude less abundant than ethane. In fact, due to its larger numbers of C-H, propane is an absorber roughly one order of magnitude more efficient than ethane.

4.3. Butane

Butane has not yet been detected, in the atmosphere of Titan. The presence of butane is predicted by photochemical models (Krasnopolsky, 2009, 2010, 2014). The quantity of butane should be lower than what it is measured and computed for propane. Available models indicate a butane mixing ratio about four order of magnitude smaller than what Krasnopolsky (2014) obtained for propane. Since no data concerning butane were found in HITRAN

and GEISA databases, we used cross-sections provided by the NIST[7]. According to this approach and taking vertical profile provided by Krasnopolsky (2014), we have checked that butane has no detectable influence on the 3.4 μm atmospheric transmittance.

4.4. Conclusion about ethane, propane, butane and others linear hydrocarbon

We have summarized our simulations results in Fig. 7, clearly the addition of propane to our set of considered gaseous species reduced the disagreement between theoretical output and solar occultation data. However, the situation is far from satisfactory, and there is room for other efficient absorbers around 3.4 microns. It is likely that other larger linear hydrocarbons are present in the atmosphere, but they are not yet retrievable from the occultation data. Moreover, their molar fractions could be very small in comparaison with the molar fraction of butane. Thus, no additional linear hydrocarbon larger than butane was considered in our model.

5. The absorption due to Polycyclic Aromatic Hydrocarbons and Hydrogenated Amorphous Carbons

As mentioned in the introduction, PAHs or more complex polyaromatic hydrocarbons like HACs (Dartois *et al.*, 2004, 2005, 2007), considered as organic compounds in solid state, are detected in the ISM (Sandford *et al.*, 1991; Pendleton & Allamandola, 2002). For instance in Dartois *et al.* (2004) the features observed in the ISM spectra fitted very well with those observed in

[7] http://webbook.nist.gov

spectra of HACs produced in laboratory (Dartois *et al.*, 2004, 2005). Furthermore, PAHs are detected on the Iapetus' and Phoebe's surface (Cruikshank *et al.*, 2008), in micro-meteorites in Antarctic (Becker *et al.*, 1997) and in the meteorite Allende (Becker & Bunch, 1997). Observations of comets reveal the presence of PAHs (Li, 2009) and in addition they were considered in Titan's upper atmosphere to explain an unidentified emission at 3.3 μm (Dinelli *et al.*, 2013; López-Puertas *et al.*, 2013). According to Bellucci *et al.* (2009) for Titan's atmosphere and Dartois *et al.* (2004, 2005, 2007); Sandford *et al.* (1991); Pendleton & Allamandola (2002) for the ISM, the features observed between 3.38 μm and 3.48 μm are due to the symmetric and asymmetric stretching of the C-H bond in -CH_2 and -CH_3 groups of the aliphatic chains. Likewise the features around 3.3 μm are signatures of stretching of aromatic C-H bond (Bellucci *et al.*, 2009; Dartois *et al.*, 2004, 2005, 2007). These latter signatures emphasize the presence of aromatic compounds like PAHs and the signatures at 3.38 μm and 3.48 μm together with the signatures of aromatic C-H stretching show the presence of complex particles containing aromatic cycles and aliphatic chains as it would expect in HACs. In Dartois *et al.* (2005), possible structures of HACs compatible with the ISM spectra were simulated with a neuronal network simulation: The resulting structure shows aromatic cycles and aliphatic chains as expected.

Thus, to clarify the observed transmission in the $3.3-3.5$ μm spectral region we considered PAHs and HACs compounds in our model.

5.1. *Polycyclic Aromatic Hydrocarbons*

The information on PAHs's transition intensities come from the NASA Ames PAHs IR Spectroscopic Database [8]. In our calculations the line widths were fixed to a reasonable value of 30 cm^{-1}. This value is approximatively comparable to the different values used for HACs (Dartois *et al.*, 2007). we introduce a correction factor $\alpha_{i,k}$ for the intensities $I_{i,k}$, with the same meaning for index i and k than the index in Eq. (4), to account for two sources of uncertainty : (1) the temperature dependence of the intensities $I_{i,k}$, (2) the uncertainties on the $I_{i,k}$'s themselves. Indeed, the spectral data provided by the Ames Database are valid for a temperature of 296 K while the actual temperature in Titan's stratosphere is substantially lower (see for instance Fig. 2a). In the spectral window of interest (*i.e.* 2700 cm^{-1}–3570 cm^{-1}), for the 716 species reported in the Ames database, we counted a total of 11, 307 calculated spectral lines against only 127 coming from an experimental determination. Even if some overlaps are present, we see that the majority of available spectral data are calculated theoretically. This rises the question of the degree of confidence that can be placed in these computed data. In this context, we have searched for theoretical and experimental spectral lines that coincide in terms of wavelength, adopting a given tolerance, respectively: 1 cm^{-1}, 2 cm^{-1} and 3 cm^{-1}. This way, we identified 52 lines that correspond to both theoretical and laboratory determinations with a tolerance of 1 cm^{-1}, 108 when is increased to 2 cm^{-1} and 144 when the tolerance is increased to 3 cm^{-1}. Consequently, we formed the log ratio $I_{\rm th}/I_{\rm exp}$ for each identified

[8] http://www.astrochem.org/pahdb/

couple of lines, with $I_{\rm th}$ the theoretical intensity and $I_{\rm exp}$ the corresponding laboratory measurement. The histograms of log ratio $I_{\rm th}/I_{\rm exp}$ values is plotted in Fig. 8. This figure shows clearly that the theoretical intensities tend to be underestimated, compared to their experimental counterparts, by a factor up to two orders of magnitude. Then, these results motivated our introduction of a factor $\alpha_{i,k}$ that represents the uncertainties that affect the spectral lines intensities available in the Ames database. In this manner, the intensity $I_{i,k}$ in Eq. (5) is replaced by the product $\alpha_{i,k}I_{i,k}$. Finally, if we combine Eq. (4) with Eq. (5), the product $\beta_{i,j,k} = x_{i,j}\alpha_{i,k}$, with the same meaning for index j than the index in Eq. (4), appears in the expression of the transmission. In first approach, we considered that the correction factors $\alpha_{i,k}$ are independent of the spectral lines. Therefore, $\beta_{i,j,k} = x_{i,j}\alpha_{i,k}$ becomes $\beta_{i,j} = x_{i,j}\alpha_i$. We took 118 neutral and charged PAHs in the Ames database. We have chosen PAHs with less than 100 carbon atoms, free of Fe, Mg, Si (not relevant for Titan's atmosphere) and for which the intensities are significant in the $3.3 - 3.5$ μm band.

5.2. Hydrogenated Amorphous Carbons

The HACs (sometimes noted a-C:H or a-C:H:N if the HACs contain nitrogen), are considered as smallest haze particle and precursor of more complex haze particle (called tholins) Lavvas *et al.* (2011) (and p. 304 of Müller-Wodarg *et al.* (2014)). In Dartois *et al.* (2004, 2005, 2007) no identified structure was given but just different vibration modes together with their vibrational frequencies or wavelengths. Analyzing the spectrum of the galaxy named IRAS 08572+3915, Dartois *et al.* (2007) fitted the intensities, wavelengths and widths of the lines for these vibration modes. Then, we use

spectrum parameters given in Table 1 of Dartois *et al.* (2007). We do not consider HACs with nitrogen (a-C:H:N) because the vibrational modes containing N are not present in $3.3 - 3.5$ μm band (Dartois *et al.*, 2005). As with PAHs, we also introduce a correction factor $\alpha_{i,k}$ on the intensities $I_{i,k}$, with the same meaning for index i and k than the index in Eq. (4), taking into account for an uncertainty source: the temperature dependence of the intensities $I_{i,k}$. Indeed, the intensities coming from the study of IRAS 08572+3915 spectrum the temperature must be different than that in Titan's stratosphere. In Dartois *et al.* (2007) no distinction was made between the different HACs but just between the vibration modes. Consequently, in our model for HACs we omit index i. Thus, our correction factor $\alpha_{i,k}$ becomes α_k and the intensities are I_k. In first approach, as with PAHs, the correction factors α_k are independent of the spectral lines. Consequently, we define a product $\beta_j = x_j \alpha$.

5.3. Results

For PAHs, $x_{i,j}$ is the molar fraction of PAHs number i with respect to the C_6H_6 abundance profile in layer j. As a first approximation, the vertical profile of this molar fraction of PAHs number i vs the C_6H_6 (used as proxy) abundance and the vertical profile of the molar fraction of HACs were kept constant. Thus for PAHs and HACs respectively, $\beta_{i,j} = x_{i,j}\alpha_i$ turns into $\beta_i = x_i \alpha_i$ and $\beta_j = x_j \alpha$ turns into $\beta = x\alpha$. Considering the uncertainties on PAHs and HACs intensities, we have fitted, respectively, the product $\beta_i = x_i \alpha_i$ and not x_i alone, and $\beta = x\alpha$ and not x, to get the best fit to occultation data. However, the resulting values do not provide information about the actual abundances of these PAHs and HACs because the problem

391 is degenerated: the correction coefficient to apply remains unknown. Taking
392 into account the log ratio $I_{\rm th}/I_{\rm exp}$ and according to the PAHs number i, we
393 obtain as best fit for β_i, values in the range of $(4.75 \times 10^{-4} - 3.32)\times$molar
394 fraction of C_6H_6. Concerning the HACs, the best fit for β is found for the
395 value 10^{-7}.
396 Fig. 9 shows that the combination of all gases, plus the 118 PAHs and HACs
397 allow a satisfactory modelization of the observed transmittance at 145 km.

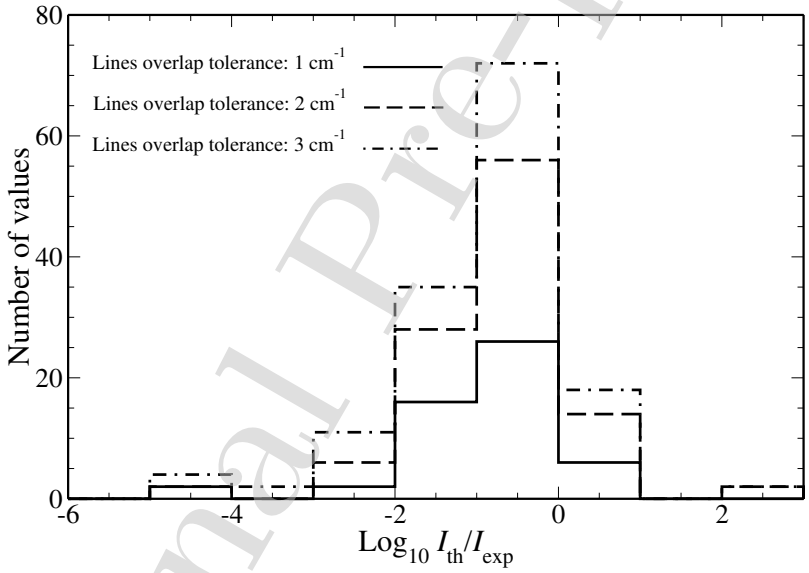

Figure 8: Histograms of the log ratios $I_{\rm th}/I_{\rm exp}$ for the Ames database PAHs for which theoretical and experimental spectral lines features determinations are available. We have considered 3 cases: (1) the wavelengths of theoretical and experimental match with a maximum tolerance of 1 cm^{-1}, (2) the same with 2 cm^{-1} and finally 3 cm^{-1}.

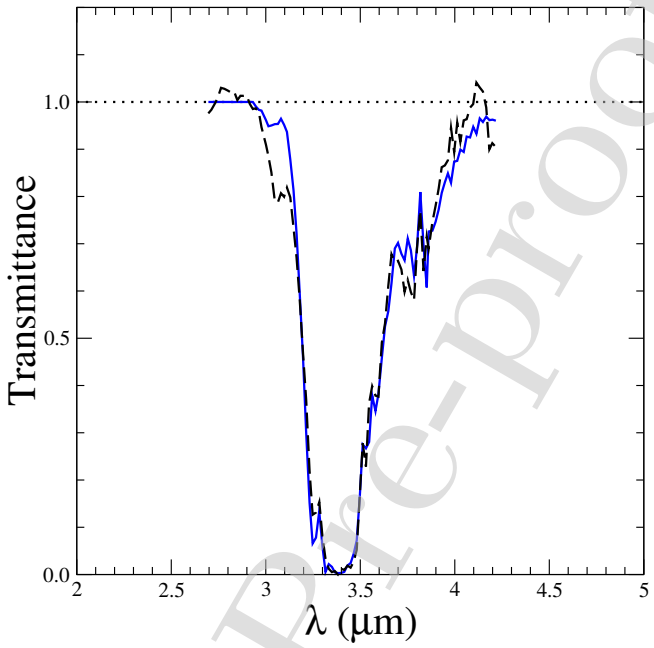

Figure 9: Computed transmittance (solid line) at 145 km during occultation T78I (observed transmittance in dash line), the radiative transfert model takes into account all studied gases plus the best fit of 118 PAHs (from NASA Ames database) and HACs (from Dartois *et al.* (2007)).

6. Discussion and Conclusion

6.1. Discussion

Observations of Saturn's stratospheric auroral regions (Guerlet *et al.*, 2015) seem to underline the remarks made on the features observed in Titan's atmosphere. Indeed, spectral signatures of benzene and aerosols in the range 680-900 cm^{-1} and 1360-1440 cm^{-1} have been observed with CIRS on

board Cassini, around the 80°S. In particular, vibrational modes in aliphatic and aromatic hydrocarbons were observed revealing the presence of PAHs or HACs in stratosphere of Saturne (Guerlet *et al.*, 2015). Moreover, as mentioned, VIMS observations of Procyon's occultation through Saturn's atmosphere around the 55°N, reported by Nicholson *et al.* (2006) and discussed by Bellucci *et al.* (2009), show similar features in the 3.4 μm band to those observed in our study. Nevertheless, the observations reveal slight differences with the Titan's 3.4 μm band spectra. But these differences could be due to a lower amount of nitrogen compounds in Saturn's atmosphere (Bellucci *et al.*, 2009). Thus, the PAHs and HACs in Titan's atmosphere could be slightly different from those in Saturn's atmosphere.

Our study of 3.4 μm band observed by solar occultation at 145 km of altitude suggests the presence of aromatic molecules like PAHs and more complex like HACs at low altitudes. Some insights can be gained by examining the results from laboratory experiments. Dartois *et al.* (2004, 2005) synthesized HACs (called a-C:H in these references) by ultraviolet photolysis of methane (Dartois *et al.*, 2004) and other hydrocarbons and nitrogen compounds to form a-C:H:N compounds (Dartois *et al.*, 2005) by UV radiation with wavelengths shorter than 120 nm in the EUV domain. Then, they made spectral Infra-Red (IR) analysis of the residues. The aim of these previous studies was to explain the spectral features observed in the ISM. Due to the presence of methane, others hydrocarbons and nitrogen compounds as well as the ultraviolet radiation in EUV domain going down to 600 km (Yoon *et al.*, 2014), the same HACs production process as in the ISM could occur in the Titan's upper atmosphere.

But this explanation is not completely satisfactory, mainly because we should find absorptions in the wavelength range 3.38 μm–3.48 μm in high altitude occultation spectra which is not the case (Courtin *et al.*, 2015). In this latter reference, the authors do not observe strong features (in extinction) in this wavelength range above 500 km but rather below 480 km (Courtin *et al.*, 2015, Fig. 2). The authors computed the ratio extinction coefficient at 3.33 μm / extinction coefficient at 3.38 μm, the wavelength at 3.33 μm being characteristic of aromatic C-H stretching and the wavelength at 3.38 μm characteristic of aliphatic C-H stretching. Thus, this ratio is function of the ratio between the aromatic and aliphatic components in the haze particles. This ratio is about 3 at 700 km and decreases to about 0.5 below 300 km. Then the conclusion of Courtin *et al.* (2015) is a growth of molecules from PAHs to more complex organics by particle-aging and coating process when the altitude decreases. So, even if the explanation in Dartois *et al.* (2004, 2005) about the HACs production in the ISM is not completely relevant for Titan's upper atmosphere, it is possible to have HACs at low altitude, by particle-aging and coating process. This process was also studied in laboratory (Carrasco *et al.*, 2018) by ultraviolet irradiation of analogs of Titan's thermosphere aerosols (and Couturier-Tamburelli *et al.* (2018)). Carrasco *et al.* (2018) analyzed the absorption peaks of residues and their time evolution. They found shifts and modifications of vibrational signatures reflecting aerosols transformation during the irradiation. The observed spectra after 24 h of irradiation appear to tend toward Titan's spectra observed in VIMS spectra at altitude 200 km. The conclusion of Carrasco *et al.* (2018) is that a particle aging process by ultraviolet irradiation occurs in Titan's atmosphere

from aerosol embryos in thermosphere to more complex haze particles in low altitudes according the following process : (1) aerosol embryos generation, (2) sedimentation and (3) chemical evolution by UV irradiation.

Other studies were conducted (Gudipati *et al.*, 2013; Yoon *et al.*, 2014). In Yoon *et al.* (2014), the authors experimentally studied the role of benzene photolysis in the PAHs and more complex particles (tholins) production. They stipulated that UV radiation with wavelengths longer than 130 nm (FUV domain) leads to the photodissociation of benzene. Likewise, in the FUV domain the photons could reach low altitudes bringing a benzene photolysis in the lower atmosphere. Then this photolysis would lead to the production of PAHs and more complex particles. In the same way, Gudipati *et al.* (2013); Couturier-Tamburelli *et al.* (2014) proceeded to photochemical experiments with C_4N_2 ice and photons in FUV domain, reproducing the environment of Titan's lower atmosphere and highlighting the fact that at low altitudes (below 200 km) the UV flux at 350 nm is comparable to the upper radiation field at shorter wavelengths. Their conclusion is that photoabsorption by haze particles in this FUV domain would trigger a rich solid-state chemistry at low altitudes. In a similar way photolysis of HC_5N led to residues containing aromatic signatures around 3.3 μm and C-H stretching around 3.4 μm (Couturier-Tamburelli *et al.*, 2015). The authors concluded that this photolysis drives the formation of more and more complex polymers which are precursors of haze particles. These results about the PAHs and HACs production at low altitudes are in agreement with our spectral analysis of the 3.4 μm band for the occultation at 145 km of altitude.

Finally, NASA has recently announced the selection of the *Dragonfly*

mission (Turtle *et al.*, 2019) as part of its *New Frontiers* program. This revolutionary quacopter is planned to explore Titan's surface, in the region of Shangri-La dune fields and Selk impact crater, during the mid-2030s. Among onboard instruments, the *Dragonfly Camera Suite* will allow PAH detection via fluorescence, excited by a controlled UV illumination (Lorenz *et al.*, 2018).

6.2. Conclusion

To conclude, the present study was to explain the strong absorption around 3.4 μm observed in the occultation spectra by VIMS at low altitudes typically lower than 450 km. We opted for the altitude 145 km which offers a good compromise : at lower altitudes, the stronger absorptions damp spectral features and at higher altitudes, the absorptions are too weak to be extracted from the signal. As a first step in our radiative transfer modeling, we have included 9 molecules following Maltagliati *et al.* (2015) : CH_4, CH_3D, CO, C_2H_2, C_2H_4, C_2H_6, H_2O, C_6H_6 and HCN. This composition leads to a poor reproduction of the observed transmittance curve. The disagreement was reduced by including C_2H_6 spectroscopic data as the data coming from Pine & Lafferty (1982) or the more exhaustive data, but empirical pseudo-line, coming from Harrison *et al.* (2010). This way, the agreement has been improved, but the simulated transmittance remained above the observed one. The inclusion of propane improved the result but there was still a lack of efficient absorbers around 3.4 μm. Knowing that spectral signatures around 3.4 μm are present in the ISM and identified as PAHs or HACs, we have considered these complex hydrocarbon compounds in our model as possible absorbers in the Titan's atmosphere at about 145 km of altitude. The fit of abundance of PAHs and HACs, taking into account some uncertainty by means of a

correction factor, allowed a rather satisfactory modelization of the observed transmittance at 145 km of altitude. Thus, the model suggests the presence of complex hydrocarbon compounds and precursors of haze particles at low altitudes. This result is also consistent with several laboratory studies showing a complexification of hydrogenated molecules from small hydrocarbons to more complex by UV irradiations (Yoon *et al.*, 2014; Couturier-Tamburelli *et al.*, 2015, 2018; Carrasco *et al.*, 2018).

References

Arking A., Grossman K. **1972**. *The Influence of the line Shape and Band Structure on Temperature in Planetary Science*. J Atmos Sci 29:937.

Becker L., Bunch T.E. **1997**. *Fullerenes, fulleranes and PAHs in the Allende meteorite*. Meteoritics and Planetary Science 32. doi:10.1111/j.1945-5100.1997.tb01292.x.

Becker L., Glavin D.P., Bada J.L. **1997**. *Polycyclic aromatic hydrocarbons (PAHs) in Antarctic Martian meteorites, carbonaceous chondrites, and polar ice* 61:475–481. doi:10.1016/S0016-7037(96)00400-0.

Bellucci A., *et al.* **2009**. *Titan solar occultation observed by Cassini/VIMS: Gas absorption and constraints on aerosol composition*. Icarus 201:198–216. doi:10.1016/j.icarus.2008.12.024.

Bézard B., Marten A., Paubert G. **1993**. *Detection of acetonitrile on Titan*. Bull Am Astron Soc 25:1100.

Bézard B., Nixon C.A., Kleiner I., Jennings D.E. **2007**. *Detection of $^{13}CH_3D$ on Titan*. Icarus 191:397–400. doi:10.1016/j.icarus.2007.06.004.

Bourgalais J., *et al.* **2016**. *Elusive anion growth in Titan's atmosphere: Low temperature kinetics of the C_3N^- + HC_3N reaction*. Icarus 271:194–201. doi:10.1016/j.icarus.2016.02.003.

Carrasco N., *et al.* **2018**. *The evolution of Titan's high-altitude aerosols under ultraviolet irradiation*. Nature Astronomy 2(6):489–494. doi:10.1038/s41550-018-0439-7.

Charnay B., *et al.* **2014**. *Titan's past and future: 3D modeling of a pure nitrogen atmosphere and geological implications*. Icarus 241:269–279. doi:10.1016/j.icarus.2014.07.009. arXiv:1407.1791.

Chou M.D., Arking A. **1980**. *Computation of Infrared Cooling Rates in the Water Vapor Bands*. J Atmos Sci 37:855.

Cordier D., *et al.* **2016**. *Structure of Titan's evaporites*. Icarus 270:4156. doi:10.1016/j.icarus.2015.12.034. arXiv:1512.07294.

Cordier D. **2016**. *How speed-of-sound measurements could bring constraints on the composition of Titan's seas*. MNRAS 459:2008–2013. doi:10.1093/mnras/stw732. arXiv:1603.07645.

Courtin R., Kim S.J., Bar-Nun A. **2015**. *Three-micron extinction of the Titan haze in the 250-700 km altitude range: Possible evidence of a particle-aging process*. A&A 573:A21.

Coustenis A., *et al.* **1998**. *Evidence for water vapor in Titan's atmosphere from ISO/SWS data.* A&A 336:L85–L89.

Coustenis A., *et al.* **2016**. *Titan's temporal evolution in stratospheric trace gases near the poles.* Icarus 270:409–420. doi:10.1016/j.icarus.2015.08.027.

Couturier-Tamburelli I., *et al.* **2014**. *Spectroscopic studies of non-volatile residue formed by photochemistry of solid C_4N_2: A model of condensed aerosol formation on Titan.* Icarus 234:81–90. doi:10.1016/j.icarus.2014.02.016.

Couturier-Tamburelli I., Piétri N., Gudipati M.S. **2015**. *Simulation of Titan's atmospheric photochemistry. Formation of non-volatile residue from polar nitrile ices.* A&A 578:A111. doi:10.1051/0004-6361/201425518.

Couturier-Tamburelli I., *et al.* **2018**. *UV-Vis Light-induced Aging of Titan's Haze and Ice.* ApJ 852:117. doi:10.3847/1538-4357/aa9e8d.

Cruikshank D.P., *et al.* **2008**. *Hydrocarbons on Saturn's satellites Iapetus and Phoebe.* Icarus 193:334–343. doi:10.1016/j.icarus.2007.04.036.

Cui J., *et al.* **2009**. *Analysis of Titan's neutral upper atmosphere from Cassini Ion Neutral Mass Spectrometer measurements.* Icarus 200:581–615. doi:10.1016/j.icarus.2008.12.005.

Dartois E., Muñoz Caro G.M., Deboffle D., d'Hendecourt L. **2004**. *Diffuse interstellar medium organic polymers. Photoproduction of the 3.4, 6.85 and 7.25 μm features* 423:L33–L36. doi:10.1051/0004-6361:200400032.

Dartois E., *et al.* **2005**. *Ultraviolet photoproduction of ISM dust. Laboratory characterisation and astrophysical relevance.* A&A 432:895–908. doi:10.1051/0004-6361:20042094.

Dartois E., *et al.* **2007**. *IRAS 08572+ 3915: constraining the aromatic versus aliphatic content of interstellar HACs.* A&A 463:635–640. doi:10.1051/0004-6361:20066572.

Dinelli B.M., *et al.* **2013**. *An unidentified emission in Titan's upper atmosphere.* Geophys. Res. Lett. 40:1489–1493. doi:10.1002/grl.50332.

Flasar F.M., *et al.* **2005**. *Titan's Atmospheric Temperatures, Winds, and Composition.* Science 308:975–978. doi:10.1126/science.1111150.

Fu Q., Liou K.N. **1992**. *On the Correlated k-Distribution Method for Radiative Transfert in Nonhomogeneous Atmospheres.* J Atmos Sci 49:2139.

Fulchignoni M., *et al.* **2005**. *In situ measurements of the physical characteristics of Titan's environment.* Nature 438:785–791. doi:10.1038/nature04314.

Gross J., Sadowski G. **2001**. *Perturbed-Chain SAFT: An Equation of State Based on a Perturbation Theory for Chain Molecules.* Ind Eng Chem Res 40:1244–1260. doi:10.1021/ie0003887.

Gudipati M.S., *et al.* **2013**. *Photochemical activity of Titans low-altitude condensed haze.* Nat. Commun. 4:1648. doi:10.1038/ncomms2649.

588 Guerlet S., *et al.* **2015**. *Stratospheric benzene and hydrocar-*
589 *bon aerosols detected in Saturn's auroral regions.* A&A 580:A89.
590 doi:10.1051/0004-6361/201424745.

591 Harrison J.J., Bernath P.F. **2010**. *Infrared absorption cross-sections for*
592 *propane (C3H8) in the 3 μm region.* JQSRT 111:1282–1288.

593 Harrison J.J., Allen N.D.C., Bernath P.F. **2010**. *Infrared absorption cross-*
594 *sections for ethane (C2H6) in the 3 μm region.* JQSRT 111:357–363.

595 Jacquinet-Husson N., *et al.* **2008**. *The GEISA spectroscopic database:*
596 *Current and future archive for Earth and planetary atmosphere*
597 *studies.* J Quant Spectrosc Radiat Transfer 109:1043–1059.
598 doi:10.1016/j.jqsrt.2007.12.015.

599 Johnson R.E., Tucker O.J., Volkov A.N. **2016**. *Evolution of an early Titan*
600 *atmosphere.* Icarus 271:202–206. doi:10.1016/j.icarus.2016.01.014.
601 arXiv:1507.08551.

602 Kim S.J., *et al.* **2011**. *Retrieval and tentative indentification of*
603 *the 3 μm spectral feature in Titan's haze.* PSS 59:699–704.
604 doi:10.1016/j.pss.2011.02.002.

605 Kim S.J., *et al.* **2012**. *The three-micron spectral feature of the Saturnian*
606 *haze: Implications for the haze composition and formation process.* PSS
607 65:122–129. doi:10.1016/j.pss.2012.02.013.

608 Koskinen T.T., *et al.* **2011**. *The mesosphere and lower thermosphere of*
609 *Titan revealed by Cassini/UVIS stellar occultations.* Icarus 216:507–534.
610 doi:10.1016/j.icarus.2011.09.022.

Krasnopolsky V.A. **2009**. *A photochemical model of Titan's atmosphere and ionosphere*. Icarus 201:226–256. doi:10.1016/j.icarus.2008.12.038.

Krasnopolsky V.A. **2010**. *The photochemical model of Titan's atmosphere and ionosphere: A version without hydrodynamic escape*. Planet. Space Sci. 58:1507–1515. doi:10.1016/j.pss.2010.07.010.

Krasnopolsky V.A. **2014**. *Chemical composition of Titan's atmosphere and ionosphere: Observations and the photochemical model*. Icarus 236:83–91. doi:10.1016/j.icarus.2014.03.041.

Lara L.M., Lellouch E., López-Moreno J.J., Rodrigo R. **1996**. *Vertical distribution of Titan's atmospheric neutral constituents*. JGR 101:23261–23283. doi:10.1029/96JE02036.

Lavvas P., Sander M., Kraft M., Imanaka H. **2011**. *Surface chemistry and particle shape: Processes for the evolution of aerosol in Titan's atmosphere*. ApJ 80:728–739. doi:10.1088/0004-637X/728/2/80.

Lavvas P., *et al.* **2015**. *N_2 state population in Titan's atmosphere*. Icarus 260:29–59. doi:10.1016/j.icarus.2015.06.033.

Lavvas P.P., Coustenis A., Vardavas I.M. **2008**a. *Coupling photochemistry with haze formation in Titan's atmosphere, Part I: Model description*. Planet Space Sci 56:27–66. doi:10.1016/j.pss.2007.05.026.

Lavvas P.P., Coustenis A., Vardavas I.M. **2008**b. *Coupling photochemistry with haze formation in Titan's atmosphere, Part II: Results and validation with Cassini/Huygens data*. Planet Space Sci 56:67–99. doi:10.1016/j.pss.2007.05.027.

Li A. **2009**. Deep Impact as a World Observatory Event: Synergies in Space, Time, and Wavelength: Proceedings of the ESO/VUB Conference held in Brussels, Belgium, 7-10 August 2006; chap. PAHs in Comets: An Overview. Berlin, Heidelberg: Springer Berlin Heidelberg; p. 161–175. doi:10.1007/978-3-540-76959-0_21.

López-Puertas M., *et al.* **2013**. *Large Abundances of Polycyclic Aromatic Hydrocarbons in Titan's Upper Atmosphere.* ApJ 770:132. doi:10.1088/0004-637X/770/2/132.

Lorenz R.D., *et al.* **2018**. *Dragonfly: A Rotorcraft Lander Concept for Scientific Exploration at Titan.* Tech. Rep. 3; Johns Hopkins APL.

Luspay-Kuti A., *et al.* **2015**. *Experimental Constraints on the Composition and Dynamics of Titan's Polar Lakes.* EPSL 410C:75–83.

Magee B.A., *et al.* **2009**. *INMS-derived composition of Titan's upper atmosphere: Analysis methods and model comparison.* Planet. Space Sci. 57:1895–1916. doi:10.1016/j.pss.2009.06.016.

Maltagliati L., *et al.* **2015**. *Titan's atmosphere as observed by Cassini/VIMS solar occultations: CH_4, CO and evidence for C_2H_6 absorption.* Icarus 248:1–24. doi:10.1016/j.icarus.2014.10.004. arXiv:1405.6324.

Moller C., Plesset M.S. **1934**. *Note on an approximation treatment for many-electron systems.* Phys Rev 46:618–622.

Müller-Wodarg I., Griffith C.A., Lellouch E., Cravens T.E. **2014**. Titan. 1st edition ed.; Cambridge Planetary Science.

Newman C.E., Richardson M.I., Lian Y., Lee C. **2016**. *Simulating Titan's methane cycle with the TitanWRF General Circulation Model*. Icarus 267:106–134. doi:10.1016/j.icarus.2015.11.028.

Nicholson P.D., Hedman M.M., Gierasch P.J., Cassini VIMS Team. **2006**. *Probing Saturn's Atmosphere with Procyon*. In: AAS/Division for Planetary Sciences Meeting Abstracts #38; vol. 38 of *Bulletin of the American Astronomical Society*. p. 555.

Nixon C.A., *et al.* **2013**. *Detection of Propene in Titan's Stratosphere*. ApJL 776:L14. doi:10.1088/2041-8205/776/1/L14. arXiv:1309.4489.

Pendleton Y.J., Allamandola L.J. **2002**. *The Organic Refractory Material in the Diffuse Interstellar Medium: Mid-Infrared Spectroscopic Constraints*. ApJS 138:75–98. doi:10.1086/322999.

Pine A.S., Lafferty W.J. **1982**. *Torsional Splittings and Assignments of the Doppler-Limited Spectrum of Ethane in the C-H Stretching Region*. Journal of Research of the National Bureau of Standards 87(3):237–256.

Poling B.E., Prausnitz J.M., O'Connell J. **2007**. The Properties of Gases and Liquids. 5th ed.; Englewood Cliffs: McGraw-Hill Professional.

Rey M., Nikitin ., Tyuterev V. **2016**. *TheoReTS An information system for theoretical spectra based on variational predictions from molecular potential energy and dipole moment surfaces*. J Mol Spectrosc 327:138–158.

Romanzin C., *et al.* **2016**. *An experimental study of the reactivity of CN^- and C_3N^- anions with cyanoacetylene (HC_3N)*. Icarus 268:242–252. doi:10.1016/j.icarus.2015.12.001.

679 Rothman L.S., *et al.* **2013**. *The HITRAN2012 molecular spec-*
680 *troscopic database.* J Quant Spectrosc Radiat Transfer 130:4–50.
681 doi:10.1016/j.jqsrt.2013.07.002.

682 Sandford S.A., *et al.* **1991**. *The interstellar C-H stretching band near 3.4*
683 *microns - Constraints on the composition of organic material in the diffuse*
684 *interstellar medium.* ApJ 371:607–620. doi:10.1086/169925.

685 Sharpe S.W., *et al.* **2004**. *Gas-Phase Databases for Quanti-*
686 *tative Infrared Spectroscopy.* Appl Spectrosc 58:1452–1461.
687 doi:10.1366/0003702042641281.

688 Tan S.P., Kargel J.S., Marion G.M. **2013**. *Titan's atmosphere and surface*
689 *liquid: New calculation using Statistical Associating Fluid Theory.* Icarus
690 222:53–72. doi:10.1016/j.icarus.2012.10.032.

691 Tan S.P., *et al.* **2015**. *Titans liquids: Exotic behavior and its*
692 *implications on global fluid circulation.* Icarus 250(0):64 – 75.
693 doi:http://dx.doi.org/10.1016/j.icarus.2014.11.029.

694 Turtle E.P., *et al.* **2019**. *Dragonfly: In Situ Exploration of Titan's Organic*
695 *Chemistry and Habitability.* In: Lunar and Planetary Science Conference.
696 Lunar and Planetary Science Conference; p. 2888.

697 Vinatier S., *et al.* **2010**. *Analysis of Cassini/CIRS limb spectra*
698 *of Titan acquired during the nominal mission. I. Hydrocarbons, ni-*
699 *triles and CO_2 vertical mixing ratio profiles.* Icarus 205:559–570.
700 doi:10.1016/j.icarus.2009.08.013.

Vinatier S., *et al.* **2015**. *Seasonal variations in Titan's middle atmosphere during the northern spring derived from Cassini/CIRS observations*. Icarus 250:95–115. doi:10.1016/j.icarus.2014.11.019.

Yoon Y.H., *et al.* **2014**. *The role of benzene photolysis in Titan haze formation*. Icarus 233:233–241. doi:10.1016/j.icarus.2014.02.006.

Acknowledgement

We thank Laurence Regalia, Bruno Bézard, Walter Lafferty and Jean Vander Auvera for scientific discussion. We are grateful to Christiaan Boersma for his kind technical help in using the NASA Ames PAH database. Finally, we warmly thank Vladimir Krasnopolsky for providing us with vertical profiles of organics.